Contamination Measurements During Operation of Hydrazine Thrusters on the P78-2 (SCATHA) Satellite

D.J. Carré* and D.F. Hall†
The Aerospace Corporation, El Segundo, California

Flight data from two hybrid retarding potential analyzer-quartz crystal microbalance detectors, one at approximately −40°C and the other at approximately −100°C, onboard the P78-2 (SCATHA) satellite were analyzed to determine if firing of eight hydrazine motors on the satellite resulted in measurable contamination at the sensors. Contamination greater than 8 ng/cm² would have been unambiguously detected. The analysis indicated that no current or mass signals that could be attributed to the firing of the hydrazine thrusters had occurred. These results provide an upper bound on contamination deposition from these thrusters at two backflow locations.

Introduction

HYDRAZINE monopropellant and bipropellant rocket motors are commonly used on spacecraft systems for attitude control; however, very little is known about hydrazine motor exhaust contamination of spacecraft surfaces that are not adjacent to the thrusters. It is possible that exhaust products condense on surfaces and react with contamination that is already present, react with the surfaces, or are altered by interaction with the spacecraft orbital environment, resulting in the degradation of spacecraft system performance.

Laboratory experiments under vacuum conditions have indicated that hydrazine thruster exhaust contamination does not collect at temperatures much above −45°C. Baerwald and Passamaneck[1] measured contamination from the firing of a 0.2-lb_f hydrazine rocket engine by means of quartz crystal microbalances (QCMs). After several thousand seconds of firing no mass accumulation was found with the QCMs at −17 and −45°C. Contaminants were detected at lower QCM temperatures and were assigned as follows: ammonia and water at −167°C, mostly water at −129°C, and aniline impurity decomposition products at −101 and −73°C. In a similar set of tests, Chirivella[2] detected no contamination from a 0.1-lb_f hydrazine rocket motor with the collecting QCMs at −18°C, although he did observe a slight (<50 monolayers) collected mass at −45°C. The QCMs of these tests were less than 31 deg from the nozzle centerline and, thus, intercepted a large flux of exhaust products. These results indicate that hydrazine rocket exhaust products do not collect on surfaces warmer than −45°C in the absence of chemical or space environmental effects such as ultraviolet radiation and particle bombardment.

The ML12 experiment on the P78-2, Spacecraft Charging at High Altitude (SCATHA) satellite, although not specifically designed for the study of hydrazine contamination, offers the opportunity for such study on orbit at locations well removed from the P78-2 thrusters. The ML12 experiment includes two sensitive temperature-controlled quartz crystal microbalance (TQCM) mass measuring devices combined with electrometers that can detect charged molecules and electrons with high sensitivity. The data from these devices have been analyzed to determine whether firing the P78-2 monopropellant hydrazine thrusters resulted in measurable contamination.

Presented as Paper 82-0079 at the AIAA 20th Aerospace Sciences Meeting, Orlando, Fla., Jan. 11-14, 1982; submitted May 14, 1982; revision received Jan. 3, 1983.

*Member Technical Staff, Chemistry and Physics Laboratory.
†Research Scientist, Chemistry and Physics Laboratory. Member AIAA.

System Description

Hydrazine Rocket Engines

The SCATHA satellite reaction control system consists of two rocket engine modules (REMs) located on the bottom of the 1.7-m-diam, 1.7-m-high, cylindrical satellite structure. Each REM has four rocket motors: two 0.23-lb_f spin engines, one 0.23-lb_f precession engine designated as a low thrust engine (LTE), and one 6.5-lb_f precession engine designated as a high thrust engine (HTE). The location of the REMs with respect to the satellite and the ML12 payload is shown in Fig. 1. The axes of the thrusters on a REM are coplanar, and the radial distance of this plane from the vehicle axis is approximately 2 cm longer than the vehicle radius.

The operational characteristics of these engines are given in Table 1. The spinup and spindown maneuvers required constant thruster operation, whereas in the LTE and HTE maneuvers, pulsed thruster operation was used. The hydrazine propellant conformed to MIL-P-2653C. The composition of the fuel is given in Table 2. Detailed analysis of the P78-2 engine performance is available in Ref. 3.

Sensors

The most sensitive instruments of the ML12 experiment are two combination sensors. Each consists of a retarding potential analyzer (RPA) for the measurement of charged molecules and electrons and a TQCM for integrated mass measurement. This arrangement permits the determination of the fraction of collected mass caused by ionic species. A cross-sectional view of the instrument is shown in Fig. 2.

Each RPA is capable of measuring ion- or electron-impact-induced currents in the 1×10^{-12} to 1×10^{-8} A range with a resolution of 1×10^{-12} A. This corresponds to 2.5×10^{6} to 2.5×10^{10} ions or electrons/(cm^2 s). The first grid is usually at the spacecraft frame potential but can be commanded to the retarding grid potential to increase the effective area of the aperture. The surrounding conductively coated radiator and conducting spacecraft surfaces minimize local perturbations to the electric field. The retarding grid can be commanded to any of the following potentials or be caused to cycle through them at 8 s/step: −100, −10, −1, 0, 1, 10, 100, and 500 V. The collector area is approximately 2.5 cm^2.

The TQCM is a 15-MHz instrument with the sensing and reference quartz crystals in tandem. The crystal electrodes are

Table 1 Operation of SCATHA RCS rocket engines[a,b]

Maneuver	Engine designations	No. of spin maneuvers	Rate, rpm	Pulse duration, s	Total thruster operation, s	Propellant usage,[c] lb/s
HTE Precession	3,7	3	62.1	0.119	89.9	4.4
HTE Precession	3,7	3	15.0	0.078	27.7	1.1
Spindown	1,5	4	—	69-437	1100.5 const	1.5
Spinup	4,8	3	—	4.5-78.5	90.5 const	
LTE Precession	2,6	4	1.10	0.319	20.7	1.4
LTE Precession	2,6	39	1.04	0.337	652.1	

[a]Ref. 3. [b]Maneuvers through Feb. 10, 1980. [c]Sum for the number of maneuvers listed.

Table 2 Hydrazine fuel compositions[a]

Constituents	Allowable	Assay
Hydrazine	98.5% min.	98.82
Water	1.0% max	0.6
Particulate	1 mg/liter max	0.0
Chloride	0.0005% max	0.0001
Aniline	0.5% max	0.38
Iron	0.002% max	0.00008
Nonvolatile residues	0.005% max	0.0003
Carbon dioxide	0.02% max	0.0003
Other volatile carbonaceous material[b]	0.02% max	0.0003

[a]Ref. 3. [b]Total either monomethylhydrazine or unsymmetrical dimethylhydrazine-alcohol.

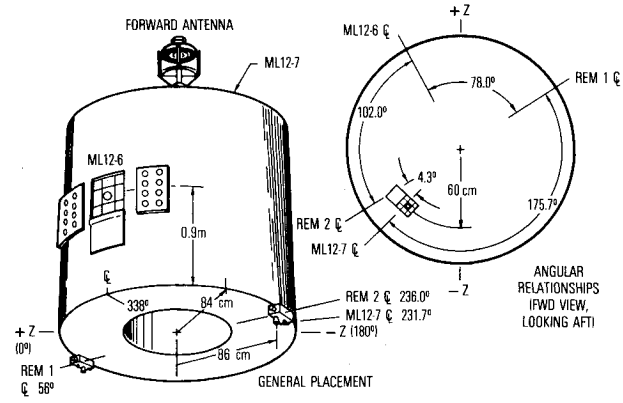

Fig. 1 Locations of ML12 TQCM/RPA sensors and hydrazine rocket engine modules on the P78-2 satellite.

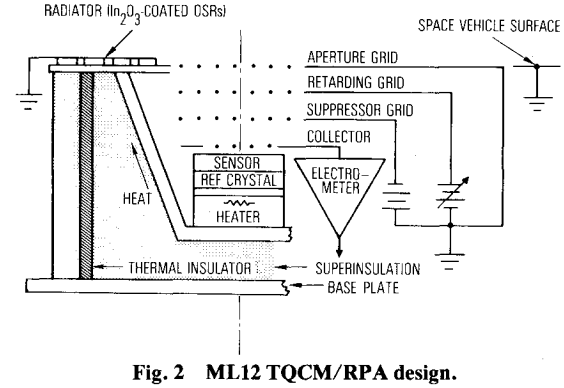

Fig. 2 ML12 TQCM/RPA design.

aluminum films. The sensitivity to collected mass is 1.56 ng/(Hz cm^2) with the frequency measured as the beat frequency between the sensing and reference crystals. When the optical density of the RPA is taken into account, the mass sensitivity is 2.4 ng/(Hz cm^2). The TQCM can be commanded to "free run" (no temperature control) or to one of the following nominal temperatures: −60, −30, 0, 30, or 100°C. (In the case of the ML12-6 TQCM, temperature control occurs 7°C below the nominal set point. Because it receives heat from the sun, ML12-6 attained a temperature of about −39°C on the free run state during the first months on orbit, whereas ML12-7 fluctuated between −90 and −100°C when continuously shadowed.) Temperature is controlled with built-in heaters, and energy is dissipated by means of thermal contact with indium oxide-coated mirror radiators. The locations on the spacecraft of the two TQCM/RPA sensors, ML12-6 and ML12-7, are shown in Fig. 1. The station of ML12-6 is approximately 0.9 m above that of the REMs; the aperture of ML12-7 is parallel to the forward end of the vehicle and about 1.7 m above the REMs.

Analysis

The satellite maneuvers involving the hydrazine thrusters are of three distinct types: major precessions of the satellite spin axis using the large thrusters (HTE), spinup and spindown maneuvers, and minor precessions using the small thrusters (LTE). The specific maneuvers chosen for analysis were those that would offer the best opportunity to detect thruster-related contamination. One HTE precession, one despin, and ten LTE precession maneuvers were analyzed. Although it was not chronologically the first of the selected maneuvers, the results of the analysis of the despin maneuver are required for the analysis of the HTE precession maneuver. Therefore, the despin maneuver is discussed first and the LTE precession maneuvers are discussed last.

Despin Maneuver

The SCATHA spin rate was reduced from 62.1 to 1.047 rpm after the spacecraft was inserted into final orbit by means of a series of maneuvers involving the spinup-spindown motors. The maneuver that reduced the spin rate from 15 to 1.5 rpm was chosen for analysis for two reasons: 1) The ML12-6 sensor cover was closed during launch and was not opened until the spin rate was 15 rpm, and 2) the maneuver was long, lasting 260 s with the thrusters firing constantly.

The mass and current data for ML12-6 are given in Figs. 3 and 4. The mass data exhibit distinctly different patterns before and after the maneuver. The patterns are the result of various cyclic events, such as differential heating of the TQCM crystals and cycling of the RPA potential and sensor heaters, which combine to give a beat frequency in the sensor output. The most important feature of these data is that the maximum value of the mass reading apparently increases by approximately 18 ng/cm^2 as a result of the maneuver. This apparent mass increase is not caused by collected contaminants, but by a frequency effect that results when sunlight periodically impinges on the sensor surface. The other factors that contribute to the observed beat patterns do not impact the ensuing analysis of the sunlight effect and the search for a true mass increase.

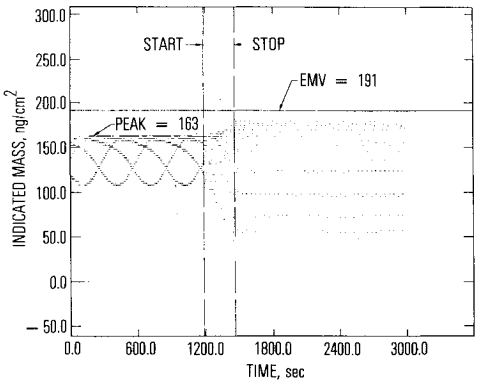

Fig. 3 ML12-6 indicated mass during despin maneuver Feb. 7, 1979 (T_0 = 45,320 s UT).

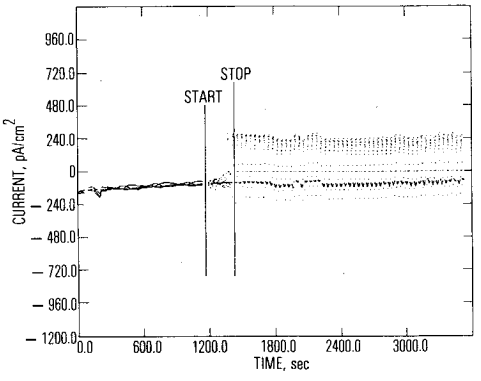

Fig. 4 ML12-6 current during despin maneuver Feb. 7, 1979 (T_0 = 45,320 s UT).

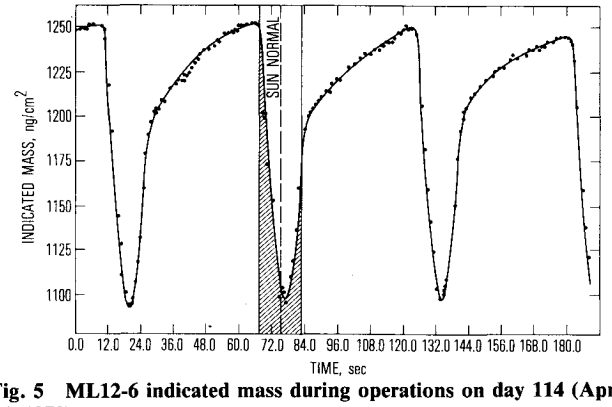

Fig. 5 ML12-6 indicated mass during operations on day 114 (April 24, 1979).

Normally, and at the time of the despin maneuver, the spacecraft is oriented with its spin axis approximately 90 deg relative to the sunlight direction. In this orientation, the ML12-6 sensor rotates in and out of the sunlight. The cyclic fluctuation in apparent mass shown in Fig. 3 is caused by repetitive heating by the sun. The response of the sensor to sunlight was characterized by analyzing data from a period of normal satellite operation. A period on April 24, 1979 (Julian day 114) was selected because the temperature of the ML12-6 sensor was within 1 deg of its temperature during despin, the vehicle spin rate was approximately 1 rpm so the response curves contained 60 points, and the data were readily available. The time constant for sensor relaxation from the sunlight perturbation obtained from these data is then used to analyze the earlier despin maneuver data.

In Fig. 5, the response of the ML12-6 sensor during day 114 is shown with the time scale expanded. A solid line through

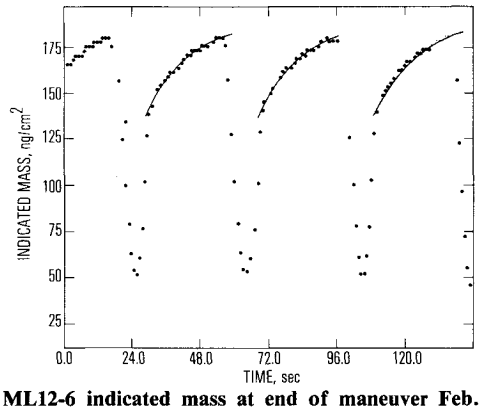

Fig. 6 ML12-6 indicated mass at end of maneuver Feb. 7, 1979 (T_0 = 46,824 s UT).

Table 3 Half-life values for sensor temperature relaxation

$t_{1/2}$, s
10.72
9.74
11.12
10.91
14.12
Average: 11.32 ±1.65

the data points and a lined area corresponding to the interval in which sunlight strikes the sensor surface have been added for clarity. When sunlight strikes the sensor surface, the apparent mass undergoes large excursions covering approximately 150 ng/cm^2. This behavior might be the result of differential heating of the sensor quartz crystals, i.e., the reference crystal temperature remains constant while the temperature of the sensing crystal varies as a function of the amount of radiation striking the sensor. The quartz crystals exhibit a dependence of frequency upon temperature.[4] Another explanation is that the sensor frequency is affected by lateral temperature gradients in the sensing crystal induced by sunlight striking near its center. We cannot distinguish between the two possibilities without laboratory work. Such work was not undertaken because the analyses of the flight data would not be affected by the mechanism of this frequency effect. When the spacecraft rotation causes the sensor to be shadowed following exposure to sunlight, the apparent mass value increases toward an equilibrium value. However, the sensor is exposed to the sunlight again before equilibrium is reached, leading to a new temperature cycle.

The observed maximum mass reading during a rotational period cannot be used as a measure of collected mass during a despin maneuver because the maximum reading depends upon the spacecraft rotational rate. On the other hand, if the mass value at sensor temperature equilibrium were attained, it would be independent of the spacecraft rotational rate and, as a result, changes in this value would be the result of true changes in the mass deposited on the sensor. This value is referred to herein as the equilibrium mass value (EMV). The experimental data indicate that the temperature relaxation to EMV is an exponential process and, as such, rate parameters derived from the data would be constant for a given equilibrium temperature. Maneuver data were analyzed by means of the Guggenheim method,[5] which yields half-lives from which the EMVs can be derived.

The Guggenheim method was used to determine the half-life value for a series of temperature relaxations during day 114. These values are listed in Table 3. The half-life corresponds to the time it takes for the change in the mass value to equal one-half the total change that the mass value

will undergo as a result of the temperature relaxation. Therefore the EMV can be estimated using the average half-life. The inaccuracy in the data used to calculate the average half-life results in an uncertainty of ± 6 ng/cm^2 in the derived EMVs.

The average value of $t_{1/2}$ was used to calculate EMVs for the data in Fig. 3. Expanded time-scale plots of the data during the despin maneuver were analyzed. Data for the latter portion of the maneuver are shown in Fig. 6. Equilibrium mass values were calculated for individual data cycles during the maneuver and they did not increase, indicating that no mass was collected as a result of the despin maneuver within the ± 6 ng/cm^2 accuracy of the method. The average EMV is 191 ng/cm^2.

The current data from ML12-6, Fig. 4, exhibit an increase in electrometer activity as a result of the maneuver. The positive current spikes occurring at a frequency corresponding to the spacecraft rotational rate indicate that photoelectron emission from the RPA collector is important. Photoemission was not detected before the despin because the electrometer output, which is sampled once per second, did not happen to be sampled during the brief time during each revolution that the sunlight was incident on the collector. Note that this pattern persists with constant amplitude following the maneuver. (The current is negative when the sensor is shadowed because a greater number of plasma electrons than plasma ions are collected.) Even if the positive currents resulted from collection of ionized contaminants by a negatively charged spacecraft, the integrated charge collected per day corresponds to a quantity of mass of the same magnitude as that normally detected by the TQCMs on days when there was no maneuver. Thus neither the mass nor current detectors located on the equatorial band of the vehicle show evidence of contamination from the spindown thrusters.

No change in current or mass values as a result of the spindown maneuver is evident in the data from ML12-7 (not shown). Since the instrument was shadowed at the time, neither signal was modulated by sunlight effects.

HTE Precession Maneuver

The large precession motors were fired several times during the early stages of the mission to orient the spacecraft for upcoming maneuvers. The HTE precession maneuver that was selected for analysis occurred with the spacecraft rotational rate at 15 rpm, two days after the opening of the ML12-6 cover. Each engine was fired for 215 pulses, resulting in the spacecraft spin axis rotating from 46 to 97 deg relative to the spacecraft-sun line.

The mass response of the ML12-6 sensor is shown in Fig. 7. Before the maneuver, an insignificant amount of sunlight impinged on the sensor surface and, as a result, there is no dependence of mass reading on spacecraft rotation. Following the maneuver, the mass response is the same as that observed for ML12-6 prior to despin from 15-1.5 rpm (Fig. 3). Since there are only four data points per revolution, the temperature relaxations and thus the EMVs cannot be measured as they were in the analysis of the despin maneuver. However, using the average EMV from the despin analysis, we can demonstrate that no mass was collected on ML12-6 during the HTE precession maneuver.

It was concluded that the despin maneuver did not result in adsorption of contamination on the ML12-6 sensor. Thus, the average EMV calculated from data following the despin maneuver should also pertain to the 15-rpm data prior to the maneuver. Note that the EMV of 191 ng/cm^2 is 28 ng/cm^2 larger than the maximum observed mass value before the despin maneuver. This relationship, the observed maximum mass value + 28 ng/cm^2 = EMV, should be valid at other times during the mission when the rotational rate, sensor temperature, and spacecraft orientation are essentially the same as the parameters preceding the despin maneuver. After the HTE precession maneuver, these conditions are met.

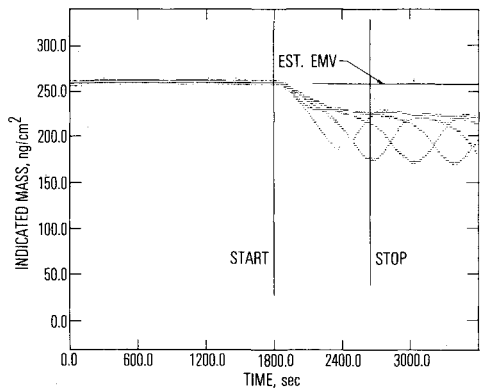

Fig. 7 ML12-6 indicated mass during HTE precession maneuver Feb. 4, 1979 (T_0 = 5401 s UT).

Table 4 LTE precession maneuvers

Date, 1979	Pulses	ML12-6 temp, °C	ML12-7 temp, °C	RPA state
March 17	25	−40	−99	0 V
April 13	49	−38	−31	Cycle
April 28	45	−8	−1	Cycle
May 5	39	−7	−1	Cycle
May 19	39	+24	+20	Cycle
June 2	39	+24	+21	Cycle
August 6	60	−38	−101	Cycle
November 27	62	−34	−99	−100 V
December 12	59	−31	−98	−10 V
December 22	63	−31	−98	−10 V

Using this relationship, the EMV derived from the post-maneuver data in Fig. 7 is 259 ng/cm^2. This value coincides with the mass reading before the maneuver, which is essentially the EMV before the maneuver because there is no rotational radiation effect on the data. (As mentioned earlier, at an angle of 46 deg between the vehicle spin axis and the sunline, sunlight does not strike the crystal surface.) Thus, no contamination was detected by the ML12-6 TQCM. The ML12-6 RPA data (not shown) support this conclusion in that there are no major current artifacts associated with the precession maneuver. There are some small current effects, probably caused by photoemission from the RPA collector, that begin approximately two-thirds through the maneuver and continue for some time after. The amplitudes of these effects were so small that they were not significant even if caused by contamination rather than photoemission.

The ML12-7 mass, temperature, and current data (not shown) for the precession maneuver were analyzed also. No effects were detected that could be attributed to sensor contamination.

LTE Precession Maneuvers

During operation in final orbit, the satellite spin axis precesses approximately 1 deg/day. To compensate for this motion, the 0.23-lb$_f$ LTE precession motors were fired once per week to maintain the spacecraft spin axis at 90 ± 5 deg with respect to the spacecraft-sun line. This spacecraft orientation places the ML12-6 sensor in the sun once per spacecraft revolution but keeps the ML12-7 sensor always in the spacecraft shadow.

For the period March 17-Dec. 22, 1979, ten LTE precession maneuvers were analyzed. The individual maneuvers were selected to give a large number of pulses and to represent various TQCM temperatures and RPA states. The maneuver specifics are given in Table 4.

Typical ML12-6 mass data are given in Fig. 8. The salient features of these data sets are the following: 1) the mass data

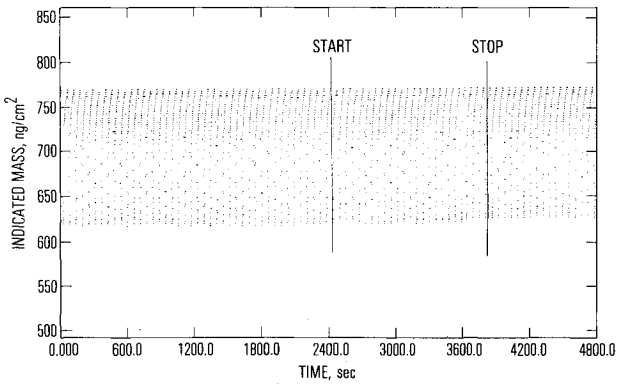

Fig. 8 ML12-6 indicated mass during LTE precession maneuver March 17, 1979 (T_0 = 9616 s UT).

for ML12-6 exhibit the cyclic behavior because of sensor heating, and 2) the maximum mass values exhibit no mass increases during the firing of the thrusters. Note that the one telemetry bit increase that begins to appear about 15 min following the conclusion of the thrust period (Fig. 8) is probably caused by the slight temperature increase of this sensor. However, since the precision of any digital measurement is never better than ±1 bit, which corresponds in this case to ±2.4 ng/cm^2, this apparent increase in mass on the crystal is not significant.

No thruster-related changes were observed in the ML12-7 mass and ML12-6 and ML12-7 charged particle detector data sets. Thus, it can be concluded that no mass or current increases resulted from the ten selected precession maneuvers in which the axial LTEs were used.

Discussion

Data from the ML12 sensors on the SCATHA satellite indicate that there has been a continuous flux of contaminants impinging upon the spacecraft surface since it attained orbit.[6,7] There is strong evidence that sunlight promotes adsorption and retention of outgassed contaminants on the ML12-6 detector. A similar process might occur with nominally volatile thruster effluents. However, the analysis of the data from the ML12-6 and ML12-7 TQCM-RPA sensors clearly indicates that no measurable contamination took place at these locations during the firing of the SCATHA RCS hydrazine thrusters. These results apply to a specific set of sensor temperatures and spacecraft configuration and orientations.

The contaminants collected by ML12-6 during normal operations, i.e., when there was no maneuver occurring, consisted of approximately 25% positively charged molecules that presumably became ionized through interaction with sunlight and the ambient plasma surrounding the spacecraft.[7] No unusual currents were detected by the RPAs during the maneuvers; therefore, the detectors were receiving an insignificant flux of ionized molecules associated with the thruster firings.

There are two possible explanations for the absence of measurable contamination: 1) the molecular flux levels associated with the thruster firings were insignificant at the sensor, or 2) there were significant flux levels of un-ionized molecules that were not measured by the sensor because they did not adhere to the sensor surfaces.

Laboratory studies involving gas nozzle plumes[8] and small thrusters,[9,10] in which most or all of the effluents were measured as a function of angle, have indicated that fluxes into the backflow region are a strong function of angle, but near the exit plane are in the general range of 10^{-4} of centerline flux values. Theory indicates that the average molecular weight of the exhaust should decrease with increasing angle from the centerline. Therefore, the flux of condensable molecules is probably less than 10^{-4} of the centerline value. When the angles and distances of the ML12 sensors from the various thrusters are considered, it seems reasonable that the arriving flux of high molecular weight molecules might have been insignificant. It would be interesting to use a plume modeling code such as CONTAM III[11] to calculate such values.

For ML12-6, on the equatorial band of the spacecraft, the second hypothesis of a flux of molecules going undetected in turn has two implications:

1) The molecules were too volatile to condense on the sensor surface. On the basis of previous laboratory studies,[1,2] molecular contaminants from hydrazine thruster operations would not be expected to condense on dark surfaces warmer than −45°C. The lowest temperature achieved by ML12-6 during maneuvers was −41°C.

2) Photochemical deposition of contaminants is not a significant mechanism for hydrazine exhaust products. Photochemical reactions have near-zero activation energies and, as a result, long surface residence times are not required for reactions to occur. Thus, if there was a substantial flux of neutral molecules, the fact that the temperature of the sensor surface was always above −45°C should not have precluded photochemical deposition.

The situation with the ML12-7 sensor is quite different from ML12-6. Since the sensor was continuously shadowed, surface photochemical reactions were not possible. However, during some of the maneuvers, the sensor temperature was approximately −100°C and some contaminant condensation was possible. The major exhaust products, N_2, H_2, and NH_3, are too volatile to condense on the −100°C surface. Unreacted hydrazine and aniline also would not be expected to accumulate, although a large flux of these species might possibly produce a transient adsorption of short duration. However, Chirivella[2] found in laboratory studies that a small quantity (<50 monolayers) of exhaust contaminant was collected at −45°C. His result implies that there are small quantities of higher molecular weight (MW > 150) species in the exhaust. At colder temperatures, the collection efficiency of this contaminant would be greater. The absence of measured thruster exhaust contaminant indicates that the higher molecular weight species did not arrive at the ML12-7 sensor in sufficient quantity to be detected. This is not surprising because ML12-7 is on the opposite end of the spacecraft from the thrusters and the contaminants would have to be turned more than 180 deg into the backflow region to impinge on the detector.

The P78-2 hydrazine thruster results are important, even though no contamination was detected. They indicate that for similar spacecraft component geometries and hydrazine thruster sizes, contamination caused by thruster operation would not be expected. The ML12-6 data demonstrate that sensitive surfaces in the equatorial region were not affected by thruster operations at a surface temperature of −41°C. The ML12-7 data indicate that the opposite end of the spacecraft from the end on which the thrusters were mounted was not contaminated by the thruster exhaust although the sensor was at −100°C.

Conclusions

Analysis of the TQCM/RPA data for the firing of the SCATHA RCS hydrazine thrusters indicates that no significant mass deposition or unusual ion currents resulted at the sensor locations. Depending upon the maneuver type, 5-8 ng/cm^2 of mass would have been unambiguously detected. If deposited as a uniform thin film, 8 ng/cm^2 would be less than 1 Å thick, which is an insignificant amount. The sensors on SCATHA are not ideally located for measuring thruster-induced contamination; however, the sensors are in similar locations to sensitive surfaces on other spacecraft. They indicate that for spacecraft of similar geometry, thruster

location, and orientation, sensitive surfaces in the equatorial band region will not be contaminated by the thrusters if they are warmer than −41°C. Sensitive surfaces on the opposite end of the spacecraft will not be contaminated at −100°C in the absence of photochemical effects. In the absence of information pertaining to the molecular flux arriving at the detectors, we cannot ascertain whether the lack of mass accumulation results from a low arrival rate or from a low sticking coefficient and lack of photochemical reactivity or other environmental effect.

Acknowledgments

This work was supported by the U.S. Air Force Wright Aeronautical Laboratory/MLBE, WPAFB, and Space Division, LAAFS, under Contract F04701-81-C-0082. Special thanks are due S. Ritter and J. Wakimoto of The Aerospace Corporation for assistance with data analysis and the mission control team (MCCF) of the Air Force Satellite Test Center for flight operations.

References

[1]Baerwald, R.K. and Passamaneck, R.S., "Monopropellant Thruster Exhaust Plume Contamination Measurements," Air Force Rocket Propulsion Laboratory, AFRPL-TR-77-44, Sept. 1977.

[2]Chirivella, J.E., "Hydrazine Engine Plume Contamination Mapping, Final Report," Air Force Rocket Propulsion Laboratory, AFRPL-TR-75-16, Oct. 1975.

[3]Berliner, E., "Design Considerations and Operational Performance of P78-2 (SCATHA) Program Reaction Control System," AIAA Paper 80-1295 presented at the AIAA/SAE/ASME 16th Joint Propulsion Conference, Hartford, Conn., June 1980.

[4]Warner, A.W. and Stockbridge, C.D., in *Vacuum Microbalance Techniques,* Vol. 2, edited by R.F. Walker, Plenum Press, New York, 1972, p. 71.

[5]Frost, A.A. and Pearson, R.G., *Kinetics and Mechanism*, 2nd ed., Wiley, New York, 1965, p. 49.

[6]Hall, D.F., "Flight Experiment to Measure Contamination Enhancement by Spacecraft Charging," *Proceedings of the Society of Photo-Optical Instrumentation Engineers*, Vol. 216, 1980, pp. 131-137.

[7]Clark, D.M. and Hall, D.F., "Flight Evidence of Spacecraft Surface Contamination Rate Enhancement by Spacecraft Charging Obtained with a Quartz Crystal Microbalance," *Proceedings of the Third AF/NASA Spacecraft Technology Conference,* Colorado Springs, Colo., NASA CP 2182, Nov. 1980, pp. 493-508.

[8]Chirivella, J.E., "Molecular Flux Measurements in the Back Flow Region of a Nozzle Plume," NASA TM 33-620, July 1973.

[9]Alt, R.E., "Bipropellant Engine Plume Contamination Program," Vol. I, Arnold Engineering Development Center, AEDC-TR-78-28, Dec. 1979.

[10]Powell, H.M., Price, L.L., and Alt, R.E., "Bipropellant Engine Plume Contamination Program," Vol. II, Arnold Engineering Development Center, AEDC-TR-79-28, Nov. 1979.

[11]Hoffman, R.J., "CONTAM Data Analysis and Model Improvement Program—The CONTAM III Computer Program," Science Applications, Inc., Los Angeles, Calif., Vol. 1-3, AFRPL-TR-82-33, April 1982, June 1982, and Mar. 1983.